ELSEVIER

Journal of Quantitative Spectroscopy & Radiative Transfer 88 (2004) 37–46

Journal of Quantitative Spectroscopy & Radiative Transfer

www.elsevier.com/locate/jqsrt

The effect of particle shape on microphysical properties of Jovian aerosols retrieved from ground-based spectropolarimetric observations

Janna M. Dlugach[a], Michael I. Mishchenko[b,*]

[a] *Main Astronomical Observatory of the National Academy of Sciences of Ukraine, 27 Zabolotny Str., 03680, Kyiv, Ukraine*
[b] *NASA Goddard Institute for Space Studies, 2880 Broadway, New York, NY 10025, USA*

Received 13 November 2003; accepted 15 March 2004

Abstract

In this paper we study potential errors in the retrieved values of the cloud particle refractive index and size that may result from the neglect of nonsphericity in analyses of ground-based spectropolarimetric observations of Jupiter. Using *T*-matrix and vector radiative-transfer codes, we have carried out numerous computations in the spectral range from 0.423 to 0.798 μm for a plane-parallel model atmosphere comprising polydisperse ensembles of randomly oriented oblate and prolate spheroids with sizes comparable to the wavelength. The particle models were specified by a gamma size distribution with varying values of the effective radius and effective variance and by a varying refractive index. Two models of the Jovian atmosphere were considered: (i) a homogeneous semi-infinite layer composed of gas and cloud particles; and (ii) a two-layered medium with a layer of pure gas on top of a semi-infinite homogeneous layer composed of gas and cloud particles. Good agreement between ground-based observational data of the brightness and the degree of linear polarization for the center of the Jovian disk and model computations was found for the following combinations of the real part of the refractive index m_{R}, the effective radius r_{eff}, and the effective variance v_{eff}: $m_{\mathrm{R}} = 1.45$, $r_{\mathrm{eff}} = 0.35\,\mu\mathrm{m}$, $v_{\mathrm{eff}} = 0.40$ for oblate spheroids with an axial ratio of $a/b = 1.3$; $m_{\mathrm{R}} = 1.50$, $r_{\mathrm{eff}} = 0.35\,\mu\mathrm{m}$, $v_{\mathrm{eff}} = 0.30$ for prolate spheroids with $a/b = 1/1.3$; $m_{\mathrm{R}} = 1.52$, $r_{\mathrm{eff}} = 0.40\,\mu\mathrm{m}$, $v_{\mathrm{eff}} = 0.35$ for oblate spheroids with $a/b = 1.5$, and $m_{\mathrm{R}} = 1.54$, $r_{\mathrm{eff}} = 0.90\,\mu\mathrm{m}$, $v_{\mathrm{eff}} = 0.30$ for prolate spheroids with $a/b = 1/1.5$. These values (especially the real part of the refractive index) differ quite

* Corresponding author. Tel.: +1-212-678-5590; Fax: +1-212-678-5622.
E-mail addresses: mmishchenko@giss.nasa.gov, crmim@giss.nasa.gov (M.I. Mishchenko).

0022-4073/$ - see front matter Published by Elsevier Ltd.
doi:10.1016/j.jqsrt.2004.03.023

significantly from those retrieved previously for the model of spherical cloud particles and emphasize nonuniqueness of remote-sensing retrievals based on the ground-based data alone.
Published by Elsevier Ltd.

Keywords: Photopolarimetric measurements; Atmospheric aerosols; Particle shape; Refractive index; Remote sensing; Atmosphere of Jupiter

1. Introduction

Over the past few decades, a large number of measurements of the intensity and the degree of linear polarization of sunlight reflected by the atmospheres of Venus, Mars, Jupiter, and Saturn have been performed both from the Earth and from spacecraft. The interest to such studies stems from the fact that polarization of light scattered by a planetary atmosphere is very sensitive to microphysical properties of atmospheric aerosols such as their size and refractive index. Following in the steps of Lyot [1], the pioneers in this field were Coffeen et al. [2] and Hansen and Hovenier [3], who studied the Venus atmosphere. Afterwards, detailed remote-sensing analyses were carried out for the atmospheres of Jupiter [4,5] and Saturn [6] as well as for dust clouds on Mars during the dust storm of 1971 [7]. Although the likely nonsphericity of cloud particles in the atmospheres of Jupiter and Saturn and dust particles in the Martian atmosphere would seem to require an explicit model assumption about the particle shape in theoretical analyses of the polarimetric observations, the particles were always assumed to be spherical. Another way of interpreting polarimetric data is to retrieve a parameterized scattering matrix, which does not depend explicitly on the particle shape, and to leave open the question of the actual microphysical parameters of aerosols. Smith and Tomasko [8] and Braak et al. [9] used this approach in their analyses of the photopolarimetric data of Jupiter obtained from Pioneers 10 and 11 as well as from the Galileo spacecraft.

It should be expected that particle nonsphericity can affect in some way the accuracy of aerosol microphysical characteristics retrieved from remote-sensing data. Therefore, there are two related important questions to address: (i) how strong can the effect of nonsphericity be on the accuracy of remote-sensing retrievals, and (ii) to what extent can the model of spherical particles be used in calculations of scattering properties of nonspherical aerosols. Note that it was shown in [10] that even moderate nonsphericity of dust-like aerosols can cause large errors in the retrieved optical thickness if satellite reflectance measurements are analyzed using the conventional Lorenz-Mie theory [11,12]. In [13], the use of the model of spheroids in analyses of measurement data for an optically thin Martian atmosphere consisting of very small particles resulted in an increase in the mean particle radius by a factor of approximately two as compared with the model of spheres. However, there are still no publications quantifying potential errors in the values of the refractive index and size retrieved from polarimetric data that can result from the neglect of nonsphericity for particles with sizes comparable to the wavelength. Therefore, the purpose of the present paper is to clarify just this issue by using the example of the Jovian atmosphere.

2. Observational data, atmosphere models, and computational techniques

A detailed analysis of ground-based observation of Jupiter using the model of spherical cloud particles was published previously [5]. As in [5], we use spectropolarimetric data for the center of the Jovian disk collected by Morozhenko [14] at wavelength of $\lambda = 0.423$, 0.452 0.504, 0.600, and 0.798 μm in the

phase angle range $0^\circ < \alpha < 11^\circ$ and the spectrophotometric data by Woodman et al. [15] obtained in the wavelenght range from 0.300 to 1.076 μm at a phase angle of $\alpha = 2^\circ$.

We have adopted simple radiative-transfer models to describe the upper Jovian atmosphere: (A) a semi-infinite homogeneous layer composed of uniformly mixed gas and cloud particles, and (B) a two-layer atmosphere in which a gas layer of optical thickness τ_g overlays a semi-infinite homogeneous layer composed of a uniform mixture of gas and cloud particles. The justification for using such simple models in analyses of ground-based observations of the center of the Jovian disk was discussed in [5].

To interpret the photopolarimetric data, it is necessary to calculate the first two components, I and Q, of the Stokes vector $\mathbf{I}$ of the reflected radiation. These are given by

$$I(-\mu, \varphi) = \mu_0 R_{11}(\mu, \mu_0, \varphi - \varphi_0), \tag{1}$$

$$Q(-\mu, \varphi) = \mu_0 R_{21}(\mu, \mu_0, \varphi - \varphi_0), \tag{2}$$

where (μ_0, φ_0) and $(-\mu, \varphi)$ specify the directions of light incidence and reflection, respectively, and R_{11} and R_{21} are elements of the 4×4 Stokes diffuse reflection matrix $\mathbf{R}$ [16]. Eqs. (1) and (2) take into account the well-known fact that the incident solar radiation is essentially unpolarized. To determine the R_{11} and R_{21} using one of the multiple-scattering techniques currently available [16], one must first calculate the elements of the single-scattering matrix $\mathbf{F}$ for the particles forming the medium.

Theoretical computations of light scattering by nonspherical particles with sizes comparable to the wavelength are very complicated. We have chosen for this study the method that was developed in [17] and is based on Waterman's T-matrix approach [18], the justification being that this method is one of the most efficient and widely used techniques for rigorous calculations of single-scattering characteristics of polydisperse nonspherical particles in random orientation (see [12,19] for details and further references). In analogy with [5], we specify particle polydispersity in terms of the simple gamma size distribution

$$f(r) = \text{constant} \times r^{(1-3v_{\text{eff}})/v_{\text{eff}}} \exp\left(-\frac{r}{r_{\text{eff}} v_{\text{eff}}}\right), \tag{3}$$

[12,16], where r is the surface-equivalent-sphere radius and r_{eff} and v_{eff} are the effective radius and effective variance of the size distribution, respectively.

The elements R_{11} and R_{21} of the diffuse reflection matrix for model A were computed by means of a numerical solution of Ambartsumian's nonlinear integral equation [20,21]. The overlaying gas layer in model B was incorporated by means of a computational algorithm based on the invariant imbedding technique as described in [22].

3. Results of model calculations and discussion

In [5], the best agreement between the observational data of the phase dependence of the degree of linear polarization $P = -Q/I$ for the center of the Jovian disk [14] and model results for spherical aerosols was found for the effective radius $r_{\text{eff}} = 0.385$ μm, the effective variance range $0.4 \leqslant v_{\text{eff}} < 0.5$, and the real part of the refractive index $m_R = 1.386$. The second and third columns of Table 1 list the spectral values of the imaginary part of the refractive index, m_I, and the single-scattering albedo, ϖ, as inferred from the reflectivity data [15] for $v_{\text{eff}} = 0.45$. Fig. 1 compares the observational polarization data for the center of the Jovian disk [14] (dots) and the best-fit numerical results for the spheres (solid curves).

Table 1
Spectral values of the imaginary part of the refractive index m_I and the single-scattering albedo ϖ for spheres and spheroids

λ (μm)	Spheres		$\varepsilon = 1.3$		$\varepsilon = 1.5$		$\varepsilon = 1/1.3$		$\varepsilon = 1/1.5$	
	m_I	ϖ	m_I	ϖ	m_I	ϖ	m_I	ϖ	m_I	ϖ
0.423	0.0012	0.987	0.0015	0.986	0.0016	0.982	0.0019	0.982	—	—
0.452	0.0010	0.990	0.0013	0.988	0.0013	0.987	0.0014	0.988	0.0005	0.988
0.504	0.0007	0.994	0.0008	0.993	0.0009	0.992	0.0010	0.992	0.0004	0.991
0.600	0.0006	0.995	0.0007	0.995	0.0008	0.994	0.0009	0.994	0.0003	0.994
0.798	0.0025	0.983	0.0032	0.980	0.0035	0.978	0.0038	0.979	0.0018	0.975

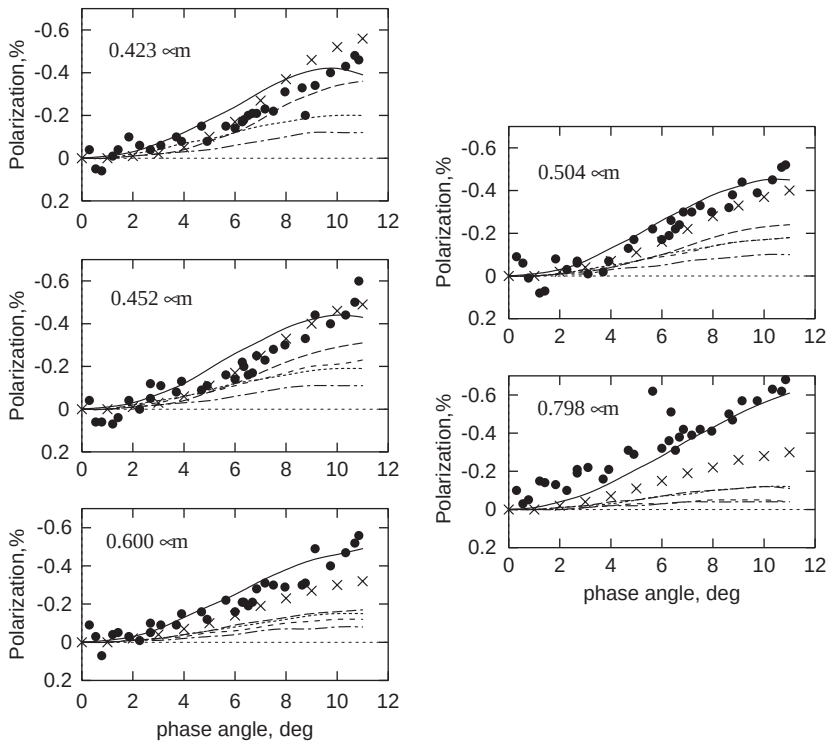

Fig. 1. Phase-angle dependence of the degree of linear polarization for the center of the Jovian disk. The dots show the observation results by Morozhenko [14]. The curves and the crosses are the results of model computations for the model A atmosphere and various cloud-particle shapes with $m_R = 1.386$, $r_{eff} = 0.385\,\mu$m, and $v_{eff} = 0.45$, as follows. Solid curves: spheres; long-dashed curves: oblate spheroids with $a/b = 1.5$; dotted curves: oblate cylinders with $D/L = 1.5$; dot–dashed curves: prolate spheroids with $a/b = 1/1.5$; short-dashed curves: prolate cylinders with $D/L = 1/1.5$; crosses: oblate spheroids with $a/b = 1.3$.

In order to extend the analysis of [5], we have chosen randomly oriented oblate and prolate spheroids and finite circular cylinders to model the likely nonsphericity of the Jovian tropospheric aerosols [23]. The shape of such particles is fully described by just one parameter (the ratio a/b of the horizontal to rotational axes for spheroids and the diameter-to-length ratio D/L for cylinders) and has been found to adequately reproduce the scattering properties of a variety of nonspherical particles [12]. Using the values of m_R, m_I, r_{eff} (expressed in terms of the surface-equivalent-sphere radius), and v_{eff} as listed above, we carried

Table 2
The ratio $I_{\text{spheroids}}(\mu = \cos\alpha,\ \mu_0 = 1)/I_{\text{spheres}}(\mu = \cos\alpha,\ \mu_0 = 1)$ for $\varepsilon = 1.5$

α (deg)	0.423 μm	0.452 μm	0.504 μm	0.600 μm	0.798 μm
0	0.99	0.99	0.99	0.99	0.99
1	0.99	0.99	0.99	0.99	0.99
2	0.99	0.99	0.99	0.99	0.99
3	0.99	0.99	0.99	0.99	0.99
4	0.99	0.99	0.99	0.99	0.99
5	0.99	0.99	0.99	0.99	0.99
6	0.99	0.99	0.99	0.99	0.99
7	0.99	0.99	0.99	0.99	0.99
8	0.98	0.98	0.98	0.99	0.99
9	0.98	0.98	0.98	0.99	0.99
10	0.97	0.98	0.98	0.98	0.99
11	0.97	0.97	0.98	0.98	0.98

out computations of the phase dependence of the degree of linear polarization for the radiation reflected by the semi-infinite layer representing model A. Note that for the center of a planetary disk, $\mu_0 = \cos\alpha$ and $\mu = 1$. The calculations were performed for two values of the axial ratio $a/b = 1.5$ (oblate particles) and $a/b = 1/1.5 = 0.666\ldots$ (prolate particles). The corresponding results are also depicted in Fig. 1. It can be seen that the results of computations for all the models of nonspherical particles considered differ substantially from the observational data as well as from the results obtained for spheres. To learn more about the effect of nonsphericity, we performed computations for oblate spheroids with $a/b = 1.3$ (crosses). As could have been expected, in this case the agreement with the observation results and with the calculations for spheres is noticeably better. Thus, we can conclude that the specific choice of aerosol shape model affects significantly the results of retrievals of particle microphysical characteristics from polarimetric measurements. As a consequence, the model parameter values derived by Morozhenko and Yanovitskii [4] and Mishchenko [5] can be expected to be inadequate if the clouds in the Jovian atmosphere consist largely of nonspherical particles.

As for the reflected intensity, our computations for the center of the Jovian disk in the range of phase angles $0° < \alpha < 11°$ show a very weak dependence of I on aerosol shape. As an example, Table 2 lists the ratio of the reflected intensity for the case of oblate spheroids with $a/b = 1.5$ to that for surface-equivalent spheres computed for the model A atmosphere. It is also known that the intensity of light reflected by a homogeneous semi-infinite atmosphere depends strongly on the single-scattering albedo but is relatively insensitive to small changes in the real part of the refractive index. Therefore, radiance data play a critical role only in the determination of the imaginary part of the refractive index.

As the next step in our analysis, we attempted to quantify the effect of particle shape on the retrieved refractive index and size distribution. For this purpose, we have performed computations for oblate and prolate, randomly oriented, polydisperse spheroids with axial ratios $a/b = 1.3$, 1.5, 1/1.3, and 1/1.5 and for various values of m_{R}, m_{I}, r_{eff}, and v_{eff}. The real part of the refractive index ranged from 1.3 to 1.8. The analysis scheme was similar to that described in [5]. First, we performed calculations at the fixed wavelength $\lambda = 0.798$ μm and, by varying the values of m_{R}, m_{I}, r_{eff}, and v_{eff}, looked for good agreement with both the radiance and the polarization data for the center of the Jovian disk. It should be remarked that moderate absorption did not affect noticeably the computed polarization. Then, using the values of

Table 3
Best-fit microphysical parameter values for various spheroidal particle models

ε	m_{R}	r_{eff} (μm)	v_{eff}
1.3	1.45	0.35	0.40
1.5	1.52	0.40	0.35
1/1.3	1.50	0.35	0.30
1/1.5	1.54	0.90	0.30

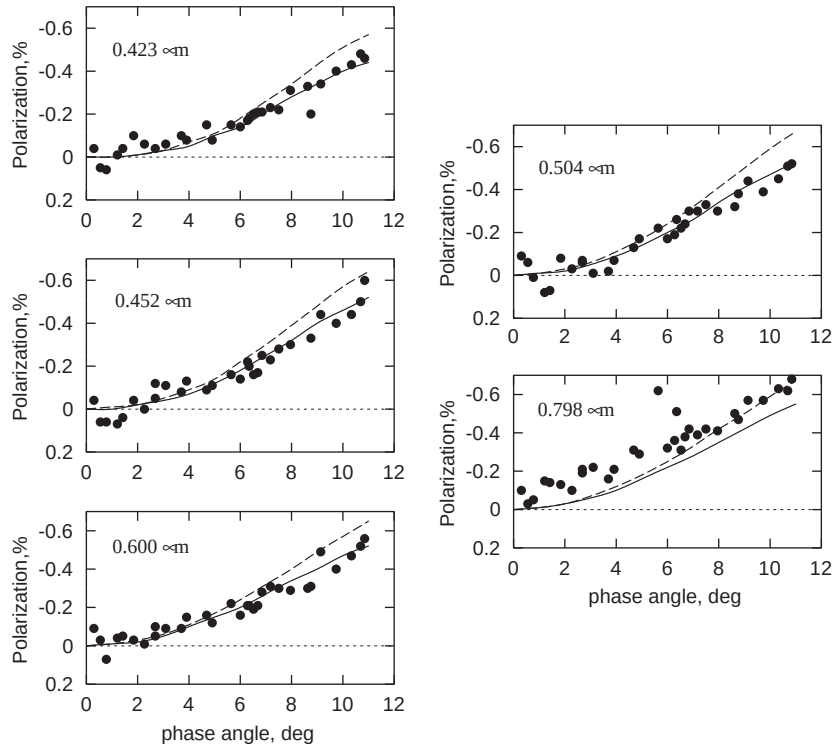

Fig. 2. Same as in Fig. 1, but for oblate spheroids with $a/b = 1.3$ and model B. Solid curves: model results for $m_{\mathrm{R}} = 1.45$, $r_{\mathrm{eff}} = 0.35\,\mu\mathrm{m}$, and $v_{\mathrm{eff}} = 0.40$. Long-dashed curves: model results for $m_{\mathrm{R}} = 1.47$, $r_{\mathrm{eff}} = 0.35\,\mu\mathrm{m}$, and $v_{\mathrm{eff}} = 0.40$.

m_{R}, r_{eff}, and v_{eff} derived at the first step, we computed polarization at $\lambda = 0.600\,\mu\mathrm{m}$. If the agreement with the observational data was satisfactory, we considered the wavelength 0.504 μm, etc. Otherwise, we returned to the wavelength 0.798 μm and repeated the procedure for new values of m_{R}, r_{eff}, and v_{eff}. This process was continued until sufficiently good agreement was found at all the wavelengths $\lambda = 0.423$, 0.452, 0.504, 0.600, and 0.798 μm.

As a result, we found that a model B atmosphere with the optical thickness of the top gaseous layer $\tau_{\mathrm{g}} = 0.2$ at $\lambda = 0.423\,\mu\mathrm{m}$ (and appropriate values at the other wavelengths consistent with the spectral behavior of the Rayleigh extinction) can reproduce the polarimetric data quite well provided that the cloud particles are spheroids with either $a/b = 1.3$ or 1.5 or 1/1.3. Similar computations for model A atmospheres were found to fit the observational data provided that the cloud particles are spheroids with

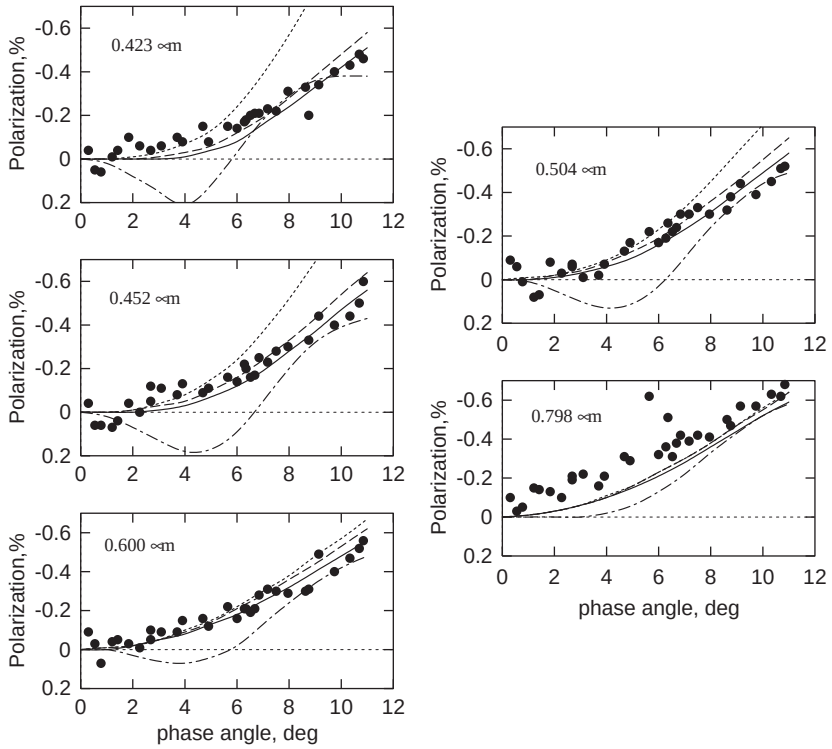

Fig. 3. Same as in Fig. 1, but for oblate spheroids with $a/b = 1.5$. Solid curves: model results for $m_R = 1.52$, $r_{eff} = 0.40\,\mu m$, and $v_{eff} = 0.35$ (model B). Dotted curves: model results for $m_R = 1.52$, $r_{eff} = 0.40\,\mu m$, and $v_{eff} = 0.35$ (model A). Long-dashed curves: model results for $m_R = 1.54$, $r_{eff} = 0.40\,\mu m$, and $v_{eff} = 0.40$ (model B). Dot-dashed curves: model results for $m_R = 1.42$, $r_{eff} = 0.80\,\mu m$, and $v_{eff} = 0.40$ (model B).

$a/b = 1/1.5$. Note that, unfortunately, the limited resources of the computer used in this study did not allow us to perform the *T*-matrix computations for such particles at the shortest wavelength $\lambda = 0.423\,\mu m$.

The resulting best-fit values of m_R, r_{eff}, and v_{eff} are listed in Table 3. The corresponding spectral values of the imaginary part of the refractive index and the single-scattering albedo retrieved by using the radiance data from [15] are given in Table 1, whereas Figs. 2–5 show the corresponding polarization phase curves. We stress that our objective was not to determine definitively and unequivocally the actual values of the cloud-particle microphysical parameters (along with the corresponding error estimates), but rather to investigate how strong is the dependence of the retrieved values on the assumed particle shape. Nevertheless, one may get a rough idea of the retrieval accuracy from Figs. 2 and 3, in which the long-dashed curves represent the results of calculations for $m_R = 1.47$, $r_{eff} = 0.35\,\mu m$, $v_{eff} = 0.40$ (Fig. 2) and $m_R = 1.54$, $r_{eff} = 0.40\,\mu m$, $v_{eff} = 0.40$ (Fig. 3). Furthermore, the dot–dashed curves in Fig. 3 depict the results of computations for $m_R = 1.42$, $r_{eff} = 0.80\,\mu m$, and $v_{eff} = 0.40$. It can be seen that in the latter case the computations agree well with the measurements at phase angles $8^\circ < \alpha < 11^\circ$, but begin to deviate significantly at smaller phase angles (where a branch of positive polarization develops), and the discrepancy only increases with decreasing wavelength. Furthermore, to demonstrate the influence of the top gaseous layer with $\tau_g = 0.2$ at $\lambda = 0.423\,\mu m$, the dotted curves in Fig. 3 depict the results of computations for the model A atmosphere with $m_R = 1.52$, $r_{eff} = 0.40\,\mu m$, and $v_{eff} = 0.35$.

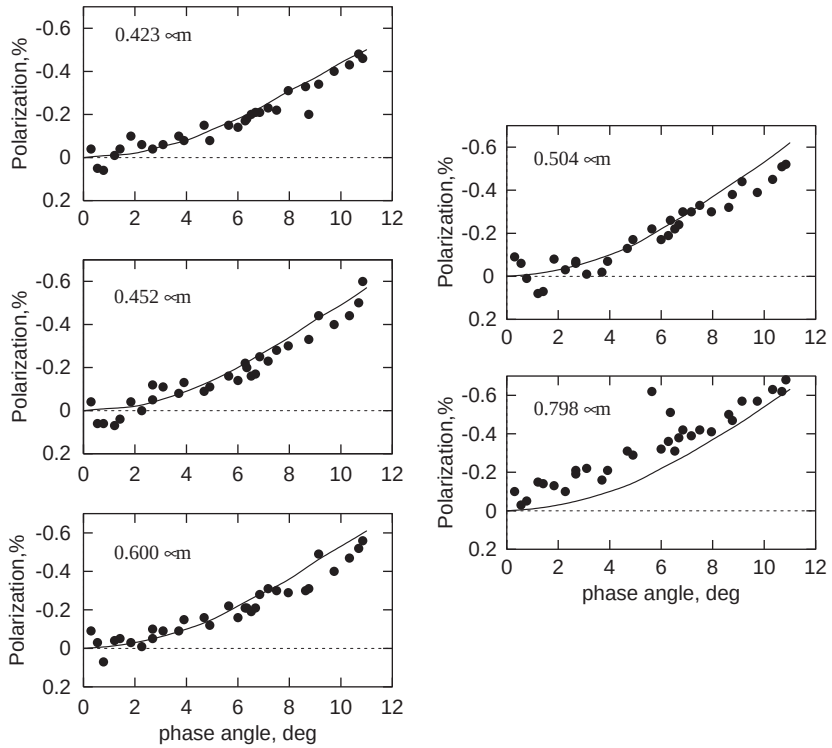

Fig. 4. Same as in Fig. 1, but for prolate spheroids with $a/b = 1/1.3$ (model B) and $m_R = 1.50$, $r_{eff} = 0.35\,\mu m$, and $v_{eff} = 0.30$ (solid curves).

Thus, the results of our calculations (Table 3) show that even weak asphericity of the assumed particle shape causes significant changes in the values of the particle microphysical characteristics as compared with those derived using the model of spheres. In the cases considered, the real part of the refractive index increases quite significantly with increasing particle asphericity. The retrieved value of the effective radius can also change by a factor exceeding 2 depending on the assumed particle shape.

It is usually believed that the Jovian troposphere is dominated by ammonia ice crystals, and that the corresponding value of the real part of the refractive index ranges from 1.441 to 1.417 for $0.453\,\mu m \leqslant \lambda \leqslant 0.940\,\mu m$ [24]. These values of the refractive index are sufficiently close to those derived by Mishchenko [5], but this agreement may not necessarily serve as a proof of sphericity of the Jovian tropospheric aerosols.

As can be seen from the data summarized in Table 3, the derived values of the real part of the refractive index (with the exception of the case $a/b = 1.3$) differ significantly from the ones mentioned above. This may be caused by the fact that spheroids are not suitable to represent the shape of the cloud particles in the Jovian troposphere. However, the nature of the Jovian cloud particles is still far from being well characterized. For example, the varied coloration of the clouds cannot be explained by the presence of pure ammonia ice and must come from an additional agent, e.g., chromophore particles mixed in with or mantled by the ammonia ice. This problem was analyzed by West et al. [23], who discussed a large number of candidates for such coloring material, but has not been resolved yet. It is clear that the presence

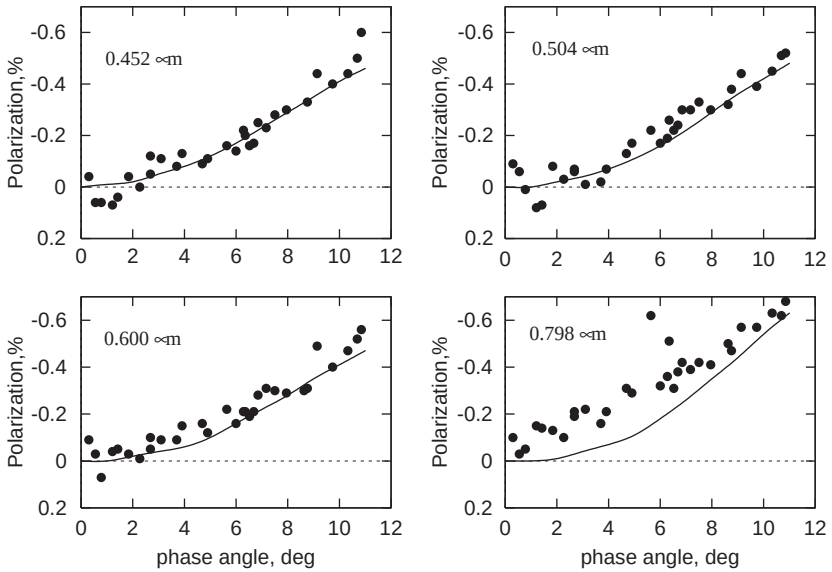

Fig. 5. Same as in Fig. 1, but for prolate spheroids with $a/b = 1/1.5$, $m_R = 1.54$, $r_{eff} = 0.90\,\mu m$, and $v_{eff} = 0.30$ (model A).

of impurities in ammonia clouds must affect the cloud particle properties, and the "effective" refractive index of the Jovian aerosols must differ in some way from the value typical of pure ammonia ice. It is thus possible that the m_R values listed in Table 3 may turn out to be relevant to the actual particles forming the tropospheric cloud layer in the Jovian atmosphere.

4. Conclusions

Using as an example the atmosphere of Jupiter, we have demonstrated that specific choice of particle shape in model computations can affect significantly the retrieval of cloud particle parameters from spectropolarimetric data. By means of *T*-matrix and multiple-scattering calculations with full account of polarization, we have found that the use of the model of polydisperse, randomly oriented spheroids results in a significant increase in the value of the real part of the refractive index as compared to that retrieved with the spherical particle model, and this discrepancy increases with increasing asphericity. Furthermore, the model of the atmosphere has to undergo a change as well. Specifically, whereas the observed polarization phase curves for the center of the Jovian disk can be reproduced by calculations for a semi-infinite homogeneous layer composed of spherical particles, the use of the model of spheroids often necessitates the introduction a two-layer model consisting of a layer of pure gas on top of a semi-infinite layer composed of gas and cloud particles.

It is thus clear that the lack of a priori information on the actual particle shape limits our ability to obtain reliable estimates of other particle microphysical parameters based on analyses of polarimetric measurements taken at a narrow range of phase angles. Furthermore, the restricted accuracy of the refractive index retrieval makes it difficult to infer the particle chemical composition. One may only hope that the availability of observational data at a wider range of phase angles can provide additional constraints on the aerosol particle model and make the inverse remote-sensing problem less ill-posed.

Acknowledgements

We thank T. Viik and an anonymous referee for their constructive comments. M. Mishchenko acknowledges financial support from the NASA Radiation Sciences Program managed by Donald Anderson.

References

[1] Lyot B. Research on the polarization of light from planets and from some terrestrial substances. NASA TT F-187. Washington, DC: NASA; 1964 .
[2] Coffeen DL, Gehrels T. Wavelength dependence of polarization. XV. Observations of Venus. Astron J 1969;74:433–45. Coffeen DL. Wavelength dependence of polarization. XVI. Atmosphere of Venus. Astron J 1969;74:446–60. Dollfus A, Coffeen DL. Polarization of Venus. I. Disk observations. Astron Astrophys 1970;8:251–66.
[3] Hansen JE, Hovenier JW. Interpretation of the polarization of Venus. J Atmos Sci 1974;31:1137–60.
[4] Morozhenko AV, Yanovitskii EG. The optical properties of Venus and the Jovian planets. I. The atmosphere of Jupiter according to polarimetric observations. Icarus 1973;18:583–92.
[5] Mishchenko MI. Physical properties of the upper tropospheric aerosols in the equatorial region of Jupiter. Icarus 1990;84:296–304.
[6] Bugaenko OI, Dlugach ZhM, Morozhenko AV, Yanovitskij EG. Optical properties of Saturn's cloud layer in the visible spectral range. Astron Vestn 1975;9:13–21 [in Russian].
[7] Dollfus A, Dlugach ZhM, Morozhenko AV, Yanovitskij EG. Optical parameters of the atmosphere and surface of Mars. II. Dust storm. Astron Vestn 1974;8:211–22 [in Russian].
[8] Smith PH, Tomasko MG. Photometry and polarimetry of Jupiter at large phase angles. II. Polarimetry of the South Tropical Zone, South Equatorial Belt, and the polar regions from the Pioneeer 10 and 11 missions. Icarus 1984;58:35–73.
[9] Braak CJ, de Haan JF, Hovenier JW, Travis LD. Galileo photopolarimetry of Jupiter at 678.5nm. Icarus 2002;157:401–18.
[10] Mishchenko MI, Lacis AA, Carlson BE, Travis LD. Nonsphericity of dust-like tropospheric aerosols: implications for aerosol remote sensing and climate modeling. Geophys Res Lett 1995;22:1077–80.
[11] van de Hulst HC. Light scattering by small particles. New York: Dover; 1981 .
[12] Mishchenko MI, Travis LD, Lacis AA. Scattering, absorption, and emission of light by small particles. Cambridge, UK: Cambridge University Press; 2002 .
[13] Dlugach ZhM, Mishchenko MI, Morozhenko AV. The effect of the shape of dust aerosol particles in the Martian atmosphere on the particle parameters. Sol Syst Res 2002;36:367–73.
[14] Morozhenko AV. Results of polarimetric investigations of Jupiter. Astrometriya Astrofiz 1976;30:47–54 [in Russian].
[15] Woodman JH, Cochran WD, Slavsky DB. Spatially resolved reflectivities of Jupiter during the 1976 opposition. Icarus 1979;37:73–83.
[16] Hansen JE, Travis LD. Light scattering in planetary atmospheres. Space Sci Rev 1974;16:527–610.
[17] Mishchenko MI. Light scattering by randomly oriented axially symmetric particles. J Opt Soc Am A 1991;8:871–82.
[18] Waterman PC. Symmetry, unitarity, and geometry in electromagnetic scattering. Phys Rev D 1071;3:825–39.
[19] Mishchenko MI, Travis LD, Mackovski DW. T-matrix computations of light scattering by nonspherical particles: a review. JQSRT 1996;55:535–75.
[20] de Rooij WA. Reflection and transmission of polarized light by planetary atmospheres. PhD thesis, Vrije Universiteit, Amsterdam, 1985.
[21] Mishchenko MI. Diffuse and coherent backscattering by discrete random media. I. Radar reflectivity, polarization ratios, and enhancement factors for a half-space of polydisperse, nonabsorbing and absorbing spherical particles. JQSRT 1996;56: 673–702.
[22] Mishchenko MI. The fast invariant imbedding method for polarized light: computational aspects and numerical results for Rayleigh scattering. JQSRT 1990;43:163–71.
[23] West RA, Strobel DF, Tomasko MG. Clouds, aerosols, and photochemistry in the Jovian atmosphere. Icarus 1986;65: 161–217.
[24] Martonchik JV, Orton GS, Appleby JF. Optical properties of NH_3 ice from the far infrared to the near ultraviolet. Appl Opt 1984;23:541–7.